

Locally Resolved ^{13}C Knight Shifts in the Organic Conductor (Fluoranthenyl) $_2\text{SbF}_6$

Michael Mehring and Jörg Spengler

Physikalisches Institut Teil 2, Universität Stuttgart, D-7000 Stuttgart 80, West Germany

(Received 4 June 1984)

Positive and negative Knight shifts of ^{13}C lines have been observed in NMR magic-angle-sample-spinning experiments on the organic conductor (fluoranthenyl) $_2\text{SbF}_6$ at room temperature. Knight-shift values (in parts per million) of 61, 42, 40, and -45 were obtained for different carbon positions; correspondingly short spin-lattice relaxation times of 75, 100, 115, and 580 ms were observed. The relevance of these data for one-dimensional conduction is discussed.

PACS numbers: 76.60.Cq, 72.15.Cz

In this Letter we will be concerned with a representative of an interesting subclass of organic conductors,¹ namely, (fluoranthenyl) $_2\text{SbF}_6$, in the following abbreviated by (FA) $_2\text{SbF}_6$, a radical cation salt, consisting of a pure hydrocarbon as organic constituent.^{2,3} The crystal structure was analyzed in detail by Enkelmann *et al.*⁴ Figure 1 shows the columnar crystal structure where the average intermolecular distance along the stack axis is 3.3 \AA . Not shown is a slight dimerization corresponding to (FA) $_2^+$ units. The dc conductivity is highest parallel to the molecular stacks, pointing at a quasi-one-dimensional behavior.³ One of the most interesting aspects of these crystals is their unique ESR properties.⁵⁻⁹ Among these the extremely narrow linewidth and corresponding long relaxation times are characteristic features which are quite unusual even for an organic "metal."

^{13}C NMR has been performed in ^{13}C -enriched tetracyanoquinodimethane in tetrathiafulvalinium tetracyanoquinodimethanide by Rybaczewski *et al.*,¹⁰ who determined the temperature dependence of the susceptibility this way. There, however, only the CN position was labeled and no local information on the conduction-band molecular orbital (MO) was obtained. In this Letter we want to present what we believe to be the first observation of locally resolved Knight shift in an organic conductor. Rapid electron motion near the Fermi surface in metals is known to cause rapid field fluctuations at the nuclear site, which result in a frequency shift (Knight shift)¹¹ and a short spin-lattice relaxation time¹² T_1 which are related by the Korringa relation:

$$K^2 T_1 T = (\hbar/4\pi k) (\gamma_e/\gamma_n)^2, \quad (1)$$

where γ_e and γ_n are the gyromagnetic ratios of the electrons and the nuclear spins, respectively, and the other symbols have their usual meaning. It should be pointed out that Eq. (1) only holds for a free-electron gas, i.e., a simple metal.

In Fig. 2 and Table I we present evidence that this unique property of conduction electrons can indeed be observed in the organic conductor (FA) $_2\text{SbF}_6$. We have performed ^{13}C high-resolution NMR experiments including magic-angle spinning ($\nu_R = 2.7 \text{ kHz}$) at the 45-MHz ^{13}C Larmor frequency¹³ (for a review of these techniques see Mehring.¹⁴) In essence all anisotropies which otherwise appear in a solid have been averaged out and the isotropic line shifts of naturally abundant (1.1%) ^{13}C in the molecular solid are observed directly. The isotropic ^{13}C shifts in liquid solutions

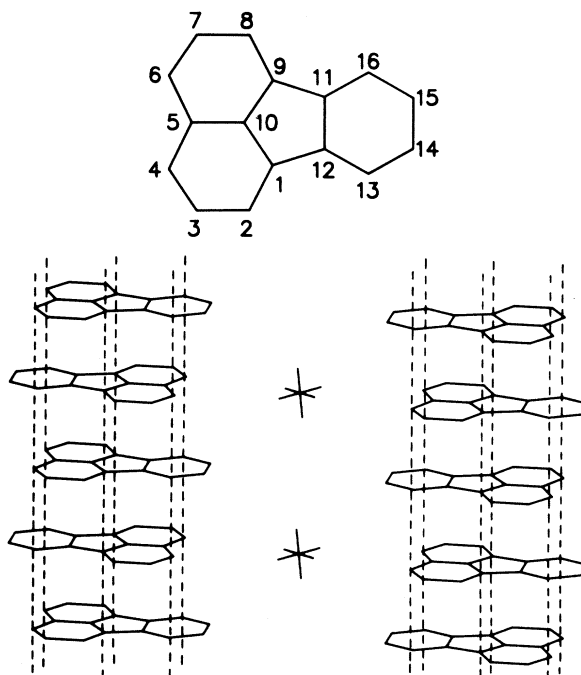


FIG. 1. Top: schematic drawing of fluoranthene molecule with the conventional numbering. Bottom: stacking of the FA molecules in the radical cation salt (Ref. 4). The intermolecular conduction path is emphasized by dashed lines. There is a slight dimerization according to (FA) $_2^+$ not shown in the figure.

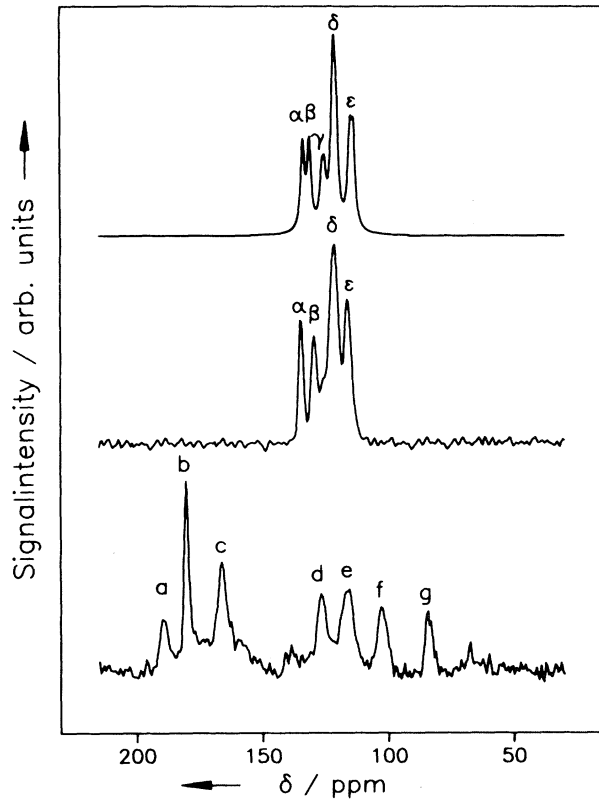


FIG. 2. Room-temperature ^{13}C NMR magic-angle-spinning spectra ($\omega_{0n}/2\pi=45$ MHz) of solid fluoranthene (middle) and of the one-dimensional conductor $(\text{FA})_2\text{SbF}_6$ (bottom). The spectrum of fluoranthene in liquid solution (top) is included for comparison.

of fluoranthene (Fig. 2, top) compare fairly well with the isotropic ^{13}C shifts in solid fluoranthene (Fig. 2, middle). The observed chemical shifts can be related to individual carbon positions in the fluoranthene molecule. The situation changes, however, drastically for fluoranthene cations in the organic conductor $(\text{FA})_2\text{SbF}_6$ (Fig. 2, bottom). Lines *a*, *b*, and *c* are clearly shifted towards the paramagnetic region (Knight shift) of the spectrum, whereas line *g* is shifted in the opposite direction (negative Knight shift). The middle part of the spectrum seems to be only slightly shifted. The Knight shift must therefore be determined with respect to the chemical shift (middle part of the spectrum). The observed shifts are on the order of 40–60 ppm [typical metal values are¹¹ 249 ppm (^7Li) and 2320 ppm (^{63}Cu)]. The corresponding relaxation times T_1 (see Table I) are much shorter than in solid fluoranthene ($T_1 > 100$ s) and scale with the Knight shift according to the Korringa relation Eq. (1).

Note that lines *a*–*g* in Fig. 2 (bottom) corre-

TABLE I. Knight shift K and spin-lattice relaxation times T_1 for lines *a*, *b*, *c*, and *g*. A tentative assignment of the lines to the carbon positions of the FA molecule (Fig. 1) is included together with the spin densities determined from K [Eq. (3)].

Line	K (ppm)	ρ_j , Eq. (3)	T_1 (10^{-3} s)	Position in FA
<i>a</i>	61	0.108	75	(4,6)
<i>b</i>	42	0.074	100	(1,9):(11,12)
<i>c</i>	40	0.072	115	(2,8)
<i>g</i>	-45	-0.07	580	(5,10)

spond to individual carbon positions in the fluoranthene cation, demonstrating that conduction occurs via the π -orbital overlap of the FA cations as sketched in Fig. 1. Although we were able to correlate all the lines α – ϵ in solid fluoranthene (Fig. 2, middle) with carbon positions of the molecule by comparing it with the liquid-solution spectrum (Fig. 2, top), we can only tentatively assign the lines *a*–*g* (Fig. 2, bottom) with carbon positions of the FA cation (see Table I). Isotopic labeling would clarify this point uniquely. Our assignment is based partly on gated decoupling experiments from which it is evident that the lines *a*, *c*, *e*, and *f* are peripheral carbon nuclei connected to protons, whereas lines *b*, *d*, and *g* are from interior carbon nuclei of the molecule not connected to protons.

The Knight shift of the NMR line of the nucleus *j* in the fluoranthene cation dimer may be expressed as

$$K_j = \chi_p (a/\hbar\gamma_e\gamma_n) \rho_j, \quad (2)$$

where χ_p is the Pauli susceptibility per $(\text{FA})_2^+$ unit, a is the isotropic part of the hyperfine tensor in radians per inverse second, and ρ_j is the spin density normalized over the $(\text{FA})_2^+$ dimer. The Pauli susceptibility can be expressed in terms of the density of states at the Fermi level per dimer $D(E_F)$ by use of the conversion formula $\chi_p = \mu_B^2 D(E_F)$, where $\mu_B = \hbar\gamma_e/2$ is the Bohr magneton. In fact χ_p was directly determined in $(\text{FA})_2\text{SbF}_6$ in comparative proton NMR and ESR investigations of the Schumacher-Slichter type.^{6,7} The value obtained is in the range $(3.1\text{--}9.4) \times 10^{-5} \text{ cm}^3 \text{ mole}^{-1}$. We use $9.4 \times 10^{-5} \text{ cm}^3 \text{ mole}^{-1}$ as an estimated value for our crystal. This amounts to $D(E_F) = 2.9 \text{ eV}^{-1}$ or, if a one-dimensional free-electron model is used with $D(E_F) = (2E_F)^{-1}$, to a Fermi energy of $E_F = 0.172 \text{ eV}$. In a tight-binding model, which seems to be appropriate for the weakly coupled p_z orbitals in $(\text{FA})_2^+X$, a bandwidth of $W = 0.34 \text{ eV}$

results which is not unreasonable. The replacement of χ_p in Eq. (2) leads to the more generally applicable expression

$$K_j = \hbar/4(\gamma_e/\gamma_n)D(E_F)a\rho_j, \quad (3)$$

where all parameters except a and ρ_j are known. In order to relate the observed Knight shift K_j at different positions to the spin density ρ_j of the conduction-band molecular orbital we have to estimate the magnitude of a . As a typical isotropic hyperfine-coupling constant a for ^{13}C nuclei in aromatic compounds we take $a/2\pi = 72$ MHz.¹⁵ Using $\gamma_e/\gamma_n = 2618$ for ^{13}C nuclei we obtain $K_j = 5.65 \times 10^{-4} \rho_j$. According to Table I the measured Knight-shift values are in the range $K = (40-64) \times 10^{-6}$, corresponding to $\rho_j = 0.07-0.1$ for the different positions j according to Eq. (3).

A very crude estimate for ρ_j would assume that the spin density is equally distributed among the 32 carbon nuclei of the FA dimer. In this case $\rho_j \approx 0.03$. The next step of analysis could involve a Hückel approach where the conduction-band MO is assumed to be the highest occupied molecular orbital (HOMO) of FA. The spin density $\rho_j = |c_j|^2$ would then be related to the HOMO coefficients, which are tabulated in the Coulson-Streitwieser compilation.¹⁶ Because of the nine nonequivalent carbon positions nine different lines should appear. In fact eight different lines are indeed observed in Fig. 2 (bottom), where supposedly some lines are overlapping. The following four largest spin densities occur in the Hückel approximation: $\rho_4 = 0.163$, $\rho_2 = 0.121$, $\rho_1 = 0.079$, and $\rho_{11} = 0.06$. All other spin densities appear to be much smaller. For the positions 5 and 10 zero spin density is found. However, it is well known that at nodes of the Hückel wave function negative spin densities usually occur in a more refined theory. If we adopt this simple view as a guideline, the following picture emerges: (i) Negative spin densities occur at positions 5 and 10 which are attributed to the negative Knight shift of line g . Note that gated decoupling experiments show that the carbon nuclei of line g are not connected to protons. (ii) The Knight-shifted lines a , b , and c are related to positions 4, 2, 1, and 11, where line b is a non-proton-connected line. This leads to the assignments in Table I. Note that line b is fairly intense. It is thus conceivable that line b is an overlapping line from four carbon positions (1, 9, 11, and 12), whereas all other lines are from two equivalent carbon positions. Line b also shows an intermediate spin density between positions 2 and 4 which deviates from the simple Hückel picture.

All spin densities from the Hückel analysis have

to be divided by a factor of 2 when compared with the data in the Table I, since we find the spin to be distributed over a dimer. Also the Hückel picture is hardly expected to be quantitatively correct; however, it seems to be helpful as a guideline to the conduction-band MO, which is after all a linear combination of the HOMO's. In a realistic band-structure calculation, however, the $(\text{FA})_2^+$ dimer should be considered to be the basic unit.

Let us now turn to the spin-lattice relaxation rate, which can be expressed as

$$T_{1j}^{-1} = n_e \rho_j^2 a^2 \left[\frac{3}{20} \epsilon J(\omega_{0n}) + \left(\frac{1}{4} + \frac{7}{20} \epsilon \right) J(\omega_{0e}) \right], \quad (4)$$

with $n_e = kT\chi_p/\mu_B^2$ and $\epsilon = d^2/a^2$, and where $J(\omega_{0n})$ is the spectral density of the fluctuating fields caused by the conduction electrons at the Larmor frequency ω_{0n} of the nuclei and $J(\omega_{0e})$ is the spectral density at the electron-spin Larmor frequency $\omega_{0e} = (\gamma_e/\gamma_n)\omega_{0n}$. The parameters a and d are the isotropic and the anisotropic part of the hyperfine tensor, respectively. The parameters which contribute to the spectral density $J(\omega)$ have been determined by pulsed ESR^{6,8} recently and can be expressed as⁸

$$J(\omega_{0n}) = \Delta a (\tau^*/D_{\parallel})^{1/2}, \quad \omega_{0n}\tau^* \ll 1, \quad (5a)$$

$$J(\omega_{0e}) = \Delta a (2D_{\parallel}\omega_{0e})^{-1/2}, \quad \omega_{0e}\tau^* \gg 1, \quad (5b)$$

where $\Delta a = 6.6 \text{ \AA}$ is the unit-cell spacing in the stacking direction, and $\tau^* = 1.6 \times 10^{-11} \text{ s}$ is the escape time from the one-dimensional diffusion parallel to the stacks with diffusion constant $D_{\parallel} = 1.3 \text{ cm}^2 \text{ s}^{-1}$. The full diffusion tensor $(D_{\parallel}, D_{\perp})$ was determined recently by the field-gradient method.^{8b} Using the parameters given here together with those used for calculating the Knight shift and $\epsilon = 1$, we obtain for $\rho_j = 0.1$ a value of $T_1 = 100 \text{ ms}$ in fair agreement with the values measured, e.g., for lines $a-c$ [see Table I; typical metal values are 150 ms (^7Li) and 3 ms (^{63}Cu)]. When one takes account of the one-dimensional nature of the electronic transport the Korringa relation [Eq. (1)] has to be modified by combining Eqs. (1)-(5) as

$$K^2 T_1 T = (\hbar/4\pi k) (\gamma_e/\gamma_n)^2 S_1, \quad (6a)$$

$$S_1 = \pi \hbar (\chi_p/\mu_B^2) \left[\frac{3}{5} \epsilon J(\omega_{0n}) + \left(1 + \frac{7}{5} \epsilon \right) J(\omega_{0e}) \right]^{-1}. \quad (6b)$$

The scaling factor ($S_1 \leq 1$) of the Korringa relation can be very small ($S_1 \ll 1$) for highly one-dimensional conductors. For a three-dimensional free-electron gas $S_1 = 1$. In our case we obtain from the

experimental data (see Table I) $S_1 \approx 10^{-2}$ and, by using Eq. (6b) together with the different parameters as given in the text, $S_1 = 2.4 \times 10^{-2}$ for $\epsilon = 1$. We remark that S_1 would be even smaller in cases where the one-dimensional escape time τ^* is longer.

Finally we mention that the recently performed Overhauser-effect measurements¹⁷ and the Overhauser shift¹⁸ are both based on the electron hyperfine interaction as discussed here. However, the spin densities should be related to the proton hyperfine interaction in those cases.

In summary, the ¹³C high-resolution NMR Knight shift and spin-lattice relaxation time in (FA)₂SbF₆ as presented here are consistent with a physical picture based on quasi-one-dimensional conduction along the (FA)₂⁺ stacks. In addition we have determined the spin-density map (see Table I) for the conduction-band molecular orbital.

We would like to acknowledge discussions with J. U. von Schütz and H. C. Wolf. One of us (M.M.) also appreciates conversations with K. P. Dinse, A. Pines, and G. Wegner. We are also grateful to M. Schwoerer and E. Dormann for sending reprints prior to publication. The Deutsche Forschungsgemeinschaft has given financial support.

¹D. Jerome and H. J. Schulz, *Adv. Phys.* **31**, 299 (1982).

²G. Wegner, *Angew. Chem.* **93**, 352 (1981).

³H. J. Keller, D. Nöthe, H. Pritzkow, D. Wehe, M. Werner, D. Koch, and D. Schweitzer, *Mol. Cryst. Liq. Cryst.* **62**, 181 (1980).

⁴V. Enkelmann, B. S. Morra, Ch. Kröhnke, and G. Wegner, *Chem. Phys.* **66**, 303 (1982).

⁵H. Eichele, M. Schwoerer, Ch. Kröhnke, and G. Wegner, *Chem. Phys. Lett.* **77**, 311 (1981).

⁶G. Sachs, W. Stöcklein, B. Bail, E. Dormann, and M. Schwoerer, *Chem. Phys. Lett.* **89**, 179 (1982); E. Dormann, *Phys. Bl.* **39**, 220 (1982); W. Stöcklein, B. Bail, M. Schwoerer, D. Singel, and J. Schmidt, *Organic Molecular Aggregates* (Springer, New York, 1983), p. 228.

⁷W. Höptner, M. Mehring, J. U. von Schütz, H. C. Wolf, B. S. Morra, V. Enkelmann, and G. Wegner, *Chem. Phys.* **73**, 253 (1982).

^{8a}G. G. Maresch, M. Mehring, J. U. von Schütz, and H. C. Wolf, *Chem. Phys.* **85**, 333 (1984).

^{8b}M. Mehring, G. G. Maresch, and J. Spengler, to be published.

⁹J. Sigg, H. Prisner, K. P. Dinse, H. Brunner, D. Schweitzer, and K. H. Hausser, *Phys. Rev. B* **27**, 5366 (1983).

¹⁰E. F. Rybaczewski, I. S. Smith, A. F. Garito, A. J. Heeger, and B. G. Silbernagel, *Phys. Rev. B* **14**, 2746 (1976).

¹¹W. D. Knight, *Solid State Phys.* **2**, 93 (1956).

¹²C. P. Slichter, *Principles of Magnetic Resonance* (Springer-Verlag, New York, 1980), pp. 116 and 148.

¹³A. Pines, M. G. Gibby, and J. S. Waugh, *J. Chem. Phys.* **59**, 569 (1973).

¹⁴M. Mehring, *Principles of High Resolution NMR in Solids* (Springer-Verlag, New York, 1983).

¹⁵K. P. Dinse, private communication.

¹⁶C. A. Coulson and A. Streitwieser, *Dictionary of π -Electron Calculation* (Pergamon, New York, 1965).

¹⁷H. Brunner, K. H. Hausser, H. J. Keller, and D. Schweitzer, to be published.

¹⁸G. Denninger, W. Stöcklein, E. Dormann, and M. Schwoerer, to be published.